MIDDLE TERM ACHIEVEMENTS OF PROJECT 5322: RETRIEVAL OF KEY ECO-HYDROLOGICAL PARAMETERS FROM REMOTE SENSING IN THE WATERSHED ALLIED TELEMETRY EXPERIMENTAL RESEARCH (WATER)

Xin Li (1), Massimo Menenti (2)

(1) Cold and Arid Regions Environmental and Engineering Research Institute of Chinese Academy of Sciences, West Donggang Road, Lanzhou, 730000, China, lixin@lzb.ac.cn
(2) Delft University of Technology,
Kluyverweg 1, 2629 HS, Delft PO Box 5058, 2600 GB Delft, The Netherlands, M.Menenti@tudelft.nl

ABSTRACT

The general objective of project 5322 in the Dragon 2 programme is to quantitatively retrieve some key eco-hydrological parameters by using remote sensed data, especially from ESA, Chinese, and the Third Party Mission (TPM). To achieve this goal, a comprehensive observation experiment, Watershed Allied Telemetry Experimental Research (WATER) was carried out. WARER is a simultaneously airborne, satellite-borne, and ground-based remote sensing experiment took place in the Heihe River Basin, a typical inland river basin in the northwest of China. This paper introduces the background and implementation of WATER. Data have been obtained so far are described in details. After a period of data analysis for two years, numerous results have also been achieved. This paper presents some early results of WATER as well.

1. INTRODUCTION

European Space Agency (ESA), together with the National Remote Sensing Centre of China (NRSCC), Ministry of Science and Technology (MOST) of China, have cooperated in the field of Earth observation application development and built the Dragon programme. The second term of Dragon Programme (Dragon 2) began in 2008 and targeted towards land, ocean and atmospheric investigations in China. Project 5322, with the title of "Key Eco-Hydrological parameters retrieval and land data assimilation system development in a typical inland river basin of China's arid region", is involved in the Dragon 2 as a hydrology theme. The goal of the project is to improve the monitoring, understanding, and predictability of hydrological and ecological processes at catchment scale, and promote the applicability of quantitative remote sensing in watershed science. Some key hydrological and ecological variables will be retrieved in virtue of ESA and other satellite data and will be merged into hydrological modeling for a more coherent and precise representation of water cycle at catchment scale. The study area is the Heihe River Basin, the second largest inland river basin in the northwest of China (Fig. 1).

This project is based on a Chinese Academy of Sciences (CAS) project -- Watershed Allied Telemetry Experimental Research (WATER) and an EU FP7 Project -- Coordinated Asia-European long-term observing system of Qinghai Tibet plateau hydro-meteorological processes and the Asian monsoon system with ground satellite image data and numerical simulations.

WATER is first of all a multi-scale land surface/hydrological experiment in a cold and arid region. Hydrological processes are very complicated, particularly in cold and arid regions, and increasingly disturbed by anthropogenic activities. However, little is known about the changes, and the hydrological, ecological and environmental impacts of these processes [1]. Land surface experiment has been proven as an effective way to promote our understandings of the terrestrial water cycle [2-5], such as HAPEX [3], HEIFE [6-7], IMGRASS [8] and NWC-ALIEX [9] for arid regions and CLPX [10] for cold regions. However, all of these experiments focused on large scale atmosphere-canopy-soil interaction with the purpose to improve GCMs and land surface models used in GCM. Other scales such as slope and mountain watershed were not considered. Therefore, in the arid and cold regions, the land surface observations, both remotely sensed and in situ, need to be significantly strengthened for a better understanding of hydrological and ecological processes at various scales. Secondly, WATER uses catchment as an integration entity. It should be able to provide reliable data for the development, improvement and verification of not only land surface models, but also distributed hydrological models and integrated watershed models. From the aspect of integrated watershed study, the lack of high-resolution, high-quality, and multi-scale data sets have been a bottleneck [11]. Therefore, the development of a multi-scale, interdisciplinary and well-coordinated

Proc. 'Dragon 2 Programme Mid-Term Results 2008 – 2010', Guilin City, People's Republic of China
17–21 May 2010 (ESA SP-684, October 2010)

experiment to observe the watershed processes at different scales is urgently needed. In this respect, WATER is a trial for establishing a watershed observing system [12]. Due to its unique natural environment, the inland river basins in northwestern China can serve as an ideal laboratory for the study of hydrological processes at catchment scale in cold and arid regions.

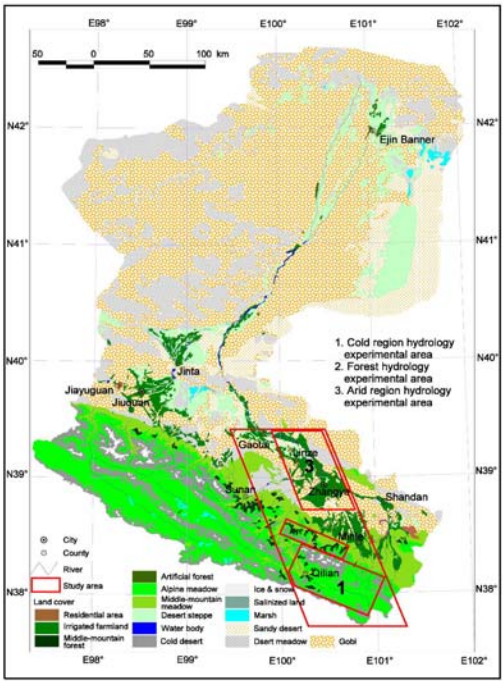

Figure 1. Heihe River Basin and the location of three key experimental areas (the background is the landscape map of the Heihe River Basin)

Evidently, satellite data acquisition is an important and necessary component both in the 5322 and the WATER projects. Project 5322 could provide huge satellite data, especially from ESA, Chinese, and the Third Party Mission (TPM) for WATER project. Meanwhile, the WATER project rewards air-borne missions and ground truths to the project 5322. This paper will introduce the background, field campaigns implementation, and particularly the progresses on parameters retrieval using both airborne and satellite-bored remote sensing data in the framework of WATER.

2. OVERVIEW OF WATER

WATER consists of the cold region, forest, and arid region hydrological experiments as well as a hydrometeorology experiment. The field campaigns have been completed, with an intensive observation period lasting from March 7 to April 12, May 15 to July 22, and August 23 to September 5, 2008, in total, 120 days. 25 airborne missions were flown. Airborne sensors including microwave radiometers at L, K and Ka bands, imaging spectrometer, thermal imager, CCD and LIDAR were used. Various satellite data were collected. Ground measurements were carried out at four scales using ground-based remote sensing instruments, densified network of automatic meteorological stations, flux towers, and hydrological stations. Based on these measurements, the remote sensing retrieval models and algorithms of water cycle variables are developed or improved, and a catchment-scale land/hydrological data assimilation system is being developed. More detailed contents can be referenced as [1].

2.1. Objectives

The overall objective of WATER is to improve the observability, understanding, and predictability of hydrological and related ecological processes at catchmental scale, accumulate basic data for the development of watershed science and promote the applicability of quantitative remote sensing in watershed science studies.

2.2. Experimental areas

The Heihe River Basin is located between 97°24′~102°10′ E and 37°41′~42°42′ N, and covers an area of approximately 130,000 km2 (Fig. 1). Landscapes of the Heihe River Basin are diverse, from the upper to downstream, glacier, frozen soil, alpine meadow, forest, irrigated crops, riparian ecosystem, desert, and gobi are distributed. WATER was implemented at four scales, namely, whole river basin, key experimental area (KEA), foci experimental area (FEA), and experiment site (ES).

2.3. Variables and parameters to be observed

The variables and parameters to be measured were identified from a viewpoint of integrated watershed model development, with reference to existing and frequently used land surface models, distributed hydrological models, and dynamic vegetation models. They were organized into five categories i.e., hydrological and ecological variables, atmospheric forcing variables, vegetation parameters, soil parameters and aerodynamic parameters. More information can be found in the detailed experiment design [13-14].

2.4. Duration

The life term of WATER was determined by the time needed for data collection and analysis. In total, four periods were determined as necessary for the implementation of WATER, they are experiment planning period, pre-observation period (POP), intensive observation period (IOP), and persistent observation period, respectively. Data processing and analysis, publication of results, and development of the WATER information system (WIS) are carried out through the implementation period of WATER, with more concentrated efforts after the IOP [1].

3. DATA

In this section, various datasets collected in the duration of WATER are briefly introduced. More details can be found in [1].

3.1. Airborne missions

The fixed-wing aircraft Y-12 (airplane ID: B-3820) was operated in WATER for the airborne missions. Seven flight regions were identified as being required, with three in the cold region, one in the forest region, and another three in the arid region hydrology experimental areas.

In total, 25 missions were flown, with 8 in the cold region, 4 in the forest region, and 13 for arid region hydrology experiment. The flying time amounted to 110 hours. Most of the airborne missions were designed to fly during the overpass of satellite sensors for concurrent analysis.

3.2. Ground data collection

1. Cold region hydrology experiment

Snow depth, density, grain size, wetness, temperature, and dielectric properties of snow were simultaneously measured using a snow fork and other instruments in Binggou watershed (BG) during the IOP. The regular observation of snowfall, evaporation, sublimation, and snow melt started with the POP. The spectral reflectance and albedo of snow were measured using an analytical spectral device (ASD) and albedometer, respectively.

Numerous ground truths were collected in A'rou (AR) and Biandukou (BDK) to verify the algorithm to detect soil freeze/thaw status and retrieve soil moisture using microwave remote sensing. The liquid soil water content and soil permittivity were measured using frequency-domain portable soil moisture probes and the gravimetric sampling method. The land surface temperature (LST) and the near surface soil temperature at 0~5cm were measured using handheld infrared thermometer and digital thermometers, respectively.

2. Forest hydrology experiment

The measurements of forest type, forest density, LAI of forest canopy, forest coverage fraction, above ground biomass of forest, forest volume density, mean forest stand height, single tree height, tree crown shape and size were carried out intensively on the ground, with most of them concurrent with airborne missions of LIDAR and CCD, or satellite overpasses of LIDAR, SAR and hyperspectral instruments.

Various field instrumentations were designed and installed to quantify the forest interception in the Guantan forest station (GT) and Pailugou (PLG). The precipitation and rainfall interception for *Picea crassifolia* were measured using rain gauges and trough gauges. The stem flow was measured by a stem flow collector.

3. Arid region hydrology experiment

Evapotranspiration (ET) was measured continuously by six eddy covariance (EC) flux towers at site scale and two large aperture scintillometer (LAS) flux systems in AR and Linze grassland (LZG) at a larger scale of 1 to a few kilometers. In addition, it was measured using microlysimeters installed in Dayekou (DYK), Yingke (YK), LZG and Linze station (LZS) during the IOP. Soil moisture was measured in LZG, LZS and BDK using the time-domain reflectometer (TDR). Due to strong salinization in LZG, the gravimetric sampling method was also used.

Leaf area index (LAI) was measured non-destructively using LAI-2000 and directly using LI-3100 and LI-3000C. The TRAC was used especially in the artificial forests. The vegetation fractional coverage was measured using the general digital camera or the special digital camera with a fisheye lens. The SunScan canopy analysis system was used to measure the fraction of photosynthetically active radiation (FPAR).

The observations of LST and emissivity on the ground were used to validate the LST retrieved from simultaneous airborne and satellite-borne thermography, which were mainly carried out in the FEAs in YK, Huazhaizi (HZZ) and LZG, and occasionally in LZS and AR.

The spectral reflectance of various vegetation was measured with wavelengths from 350-2500 nm using the ASD spectrometer. The leaf reflectance and transmittance were measured using a LI-1800-12S external integrating sphere or an ASD leaf clip. BRDF was measured using a newly designed goniometer, which can view the canopy in the upper hemisphere at a maximum height of 5m.

4. Hydrometeorology experiment

A network of hydrometeorological and flux observations was established in the upper and middle reaches of the Heihe River Basin, which was composed of AMSs, EC systems, LAS, and 8 Chinese Meteorological Administration (CMA) operational meteorological stations, and 34 CMA regional meteorological stations. Three-year continuous data were obtained in most of the stations.

The X-band dual-linear polarization Doppler weather radar mounted on a truck, with a horizontal resolution of 150 m, was employed during the IOP of WATER to obtain high resolution observations of precipitation. Two precipitation particle drop size analyzers and a number of rain gauges were installed during the IOP in the cold region, arid region and forest hydrology experimental areas, respectively.

The runoff observations in WATER were operated by the local hydrological stations. Irrigation data were collected with the cooperation of local water management bureau. Groundwater levels were monitored on a daily basis using 36 existing wells in middle reaches of the Heihe River Basin.

During the IOP, the air temperature and humidity profiles and aerosol properties were measured concurrently with airborne missions and satellite overpasses. The atmospheric sounding was carried out using the digital sounder. The optical properties of atmosphere, particularly those of aerosol were measured using CE318 sun-photometers.

3.3. Satellite data acquisition

Various satellite remote sensing data from VNIR, thermal infrared, active microwave, passive microwave, and LIDAR sensors were collected by data sharing programs (such as Dragon programme), international cooperation and a limited commercial purchase. The high resolution satellite data acquired during the POP and IOP were estimated to be above 200 scenes, and the medium and coarse resolution remote sensing data were obtained on a daily basis. The satellite data acquired in WATER are listed in Tab.1.

4. PROGRESSES ON KEY ECO-HYDROLOGICAL PARAMETER RETRIEVAL

4.1. Cold region hydrology

1. Snow properties

The snow water equivalent (SWE), snow depth (SD), snow cover area (SCA), albedo, and snow temperature are very important for snow runoff model in mountainous areas of cold region. SD and SWE were derived using k (18.7 GHz) and Ka-bands (36 GHz) microwave radiometers. The airborne experiment of SWE was implemented on 29 March, 2008. The microwave emission model of layered snowpacks (MEMLS) was adopted to simulate the brightness temperature of snow cover for each measurement point. The TBs simulated by MEMLS (using ground-based snow properties as input) were compared with the observations from radiometers on the aircraft in four sites. The deviation was less that 10 Kelvins.

As for the retrieval of SD and SWR, an empirical method was used in the first step. Second order polynomial equations were applied to fit the SD and SWE with brightness temperature differences (TBD) [15]. Data from 78 snow pits were used to calibrate the following relationships, which are

$$SD = 0.0129*TBD2+0.114*TBD+1.2723 \quad (1)$$

$$SWE = 0.0017*TBD2+0.1388*TBD-1.2 \quad (2)$$

Fig. 3 shows the estimation result of SD and SWE in the Binggou watershed. The mean SD is about 15.5 cm with a large spatial variations (standard deviation of 12.0 cm), and the maximum of SD reaches up to 84 cm. Deep snowpacks distribute on the valley with the aspect of north slope, while shallow snow covered the flat on the top and the south-oriented slope.

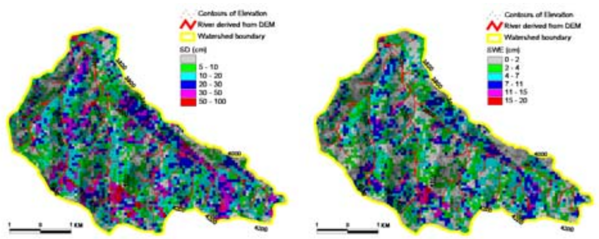

Snow depth   Snow water equivalent

Figure 3. Estimates of snow depth and snow water equivalent using airborne K and Ka bands microwave radiometry

Hyperion image at the Qilian mountainous area on March 17, 2008 was used to retrieve the snow albedo. Fig. 4 shows the retrieved result is smaller than the ground measurement at narrow bands. The error is probably caused by the considerably high albedo of snow and the mismatch of the scales between point measurements and pixel estimates [16].

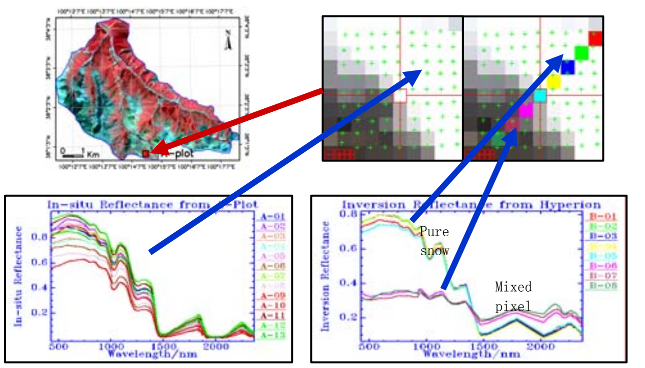

Measured spectral reflectance of snow   Estimated spectral reflectance of snow

Figure 4. Estimation of snow albedo using Hyperion data

2. Soil freeze/thaw status and soil moisture

Microwave radiometry is capable of detecting surface soil freeze and thaw. In WATER, we carried out both ground and airborne experiments in this regard. Fig. 5 illustrates the finding from a track-mounted radiometer experiment. What can be identified from the figure is that: (1) when soil temperature is below the freezing point, emissivity is relatively higher because frozen soil has a low dielectric constant. (2) When soil is thawed in daytime, liquid water content increases so that dielectric constant of soil increases accordingly. This results in a sharp decrease of emissivity of soil [17].

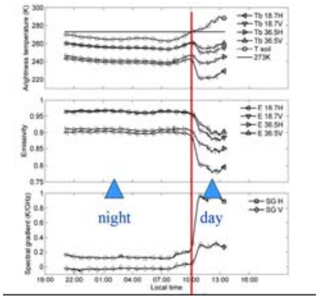

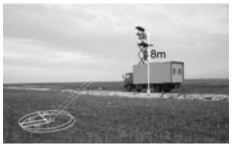

Track-mounted passive microwave radiometer

Observed brightness temperature, calculated emissivity and spectral gradient of snowfree grassland in AR, March 10-11, 2008, 50° incidence angle

Figure 5. Brightness temperature observations by ground-based radiometer at A'rou, cold region hydrology experimental area

On April 1 2008, two airborne missions were conducted in morning (7 am local time), when the soil is still frozen in the surface, and 1 pm in the afternoon, when surface soil is thawed. Fig. 6 clearly illustrates that the brightness temperature in the afternoon is significantly lower than that in the morning, suggesting that it is very feasible to detect the freeze and thaw status of surface soil using microwave remote sensing.

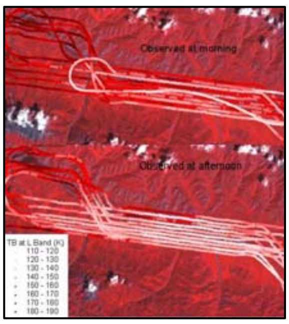

Airborne L-band data obtained on April 1, 2008

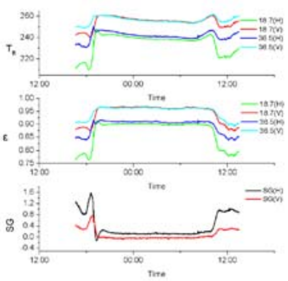

Brightness temperature, emissivity and spectral gradient for soil freeze/thaw cycle, March10-11, A'rou

Figure 6. Detection of surface soil freeze/thaw status using passive microwave radiometer

Ground penetrating radar (GPR) is an efficient method for accurate mapping heterogeneities of soil moisture at the field scale. From March to May, 2008, GPR measurements were carried out using a two 250 MHz RAMAC/GPR transmitter-receiver system. Fig.7 shows the filed scale measurement of soil moisture and frozen/thaw penetration depth using GPR. It can be concluded that GPR could be used as an optimal tool to extend point measurements of near-surface water contents to the field scale through offering a promising way for providing ground truth for remote sensing applications while at the same time giving access to auxiliary information [18].

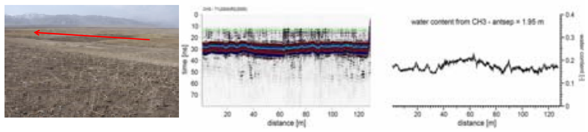

Soil moisture measurement in BDK using GPR

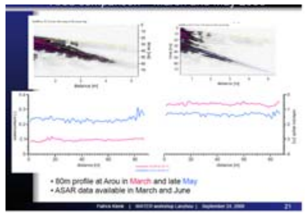

Seasonal change of soil moisture and frozen/thaw penetration depth in AR

Figure 7. Filed scale measurement of soil moisture and frozen/thaw penetration depth using GPR

4.2. Arid region hydrology

1. ET

A Two-layer Surface Energy Balance Parameterization Scheme (TSEBPS) is proposed for the estimation of surface heat fluxes using Thermal Infrared (TIR) data over sparsely vegetated surface. TSEBPS is based on the theory of the classical two-layer energy balance model, as well as a set of new formulations derived from assumption of the energy balance at limiting cases. The canopy sensible and latent heat fluxes predicted versus the measured values are shown in Fig. 8. On the whole, TSEBPS estimated sensible and latent heat fluxes agree very well with the field measurement [19]. A unique feature of TSEBPS is that it can take advantage of using multi-angular thermal infrared remote sensing data, which were obtained in WATER by the Wide-angle infrared Dual-mode line/area Array Scanner (WiDAS) [20].

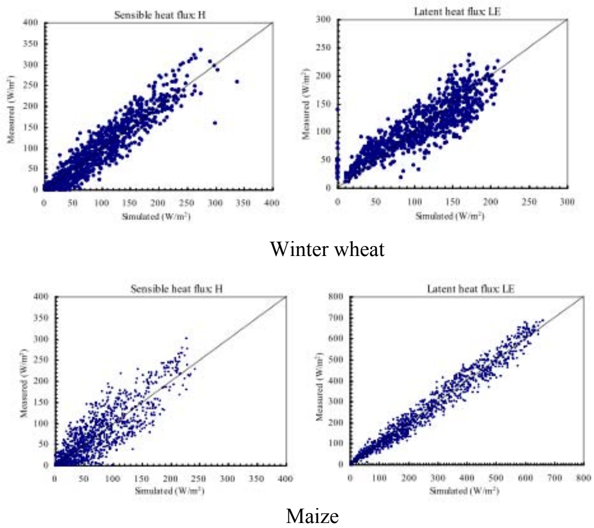

Figure 8. Comparison between observations and TSEBPS modeled sensible and latent heat fluxes over winter wheat and maize canopy

For ET estimation, roughness length (z0m) of land surfaces is an essential variable for the parameterisation of momentum and heat exchanges. The growing interest about the estimation of the surface energy balance components from passive remote sensing lead to an increasing development of models. Satellite and airborne imaging LIDAR systems have paved the way to the mapping of vegetation properties over vegetated areas. An investigation was aiming at exploring the use of imaging LIDAR measurements for the estimation of the aerodynamic roughness length over a heterogeneous landscape of the Heihe River Basin. LIDAR points were used to extract a Digital Surface Model (DSM) and a Digital Elevation Model (DEM) from a single flight pass over an irrigated area covered by field crops, small trees arrays and tree hedges, with a ground resolution of 1 meter and a total surface of 7.2 km^2. Fig. 9 shows a 3D rendering of the YK area obtained by combination of the LIDAR DSM and the high resolution image simultaneously acquired by the CCD camera and Fig. 10 illustrates the derived roughness length [21].

Figure 9. Realistic virtual scene of the YK site by combination of the LIDAR DSM and the high resolution image acquired by the CCD camera

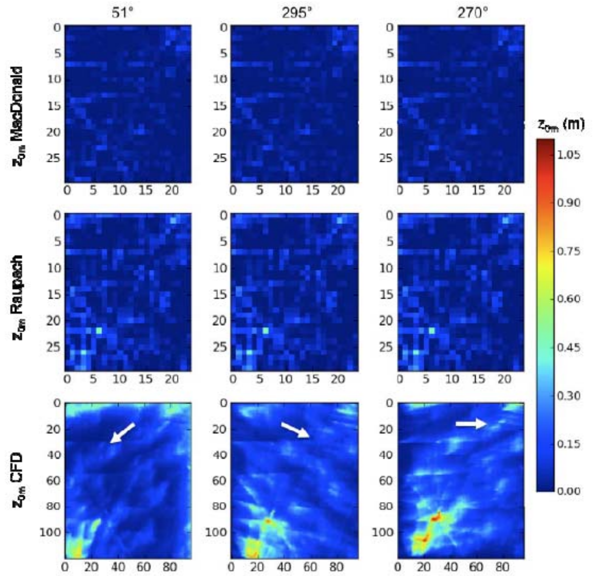

Figure 10. Roughness length maps derived from the LIDAR data over the Yingke area for wind flows from N-E , W-NW , and W

2. Soil moisture

A two-step retrieval scheme was proposed to acquire surface roughness based solely on multi-angle ASAR data, and the estimated roughness could further be used in the advanced integrated equation model (AIEM) [22-23] to retrieve surface soil moisture. This study was performed at Linze Grassland Station. Fig. 11 shows the subsets of the processed images from different swaths (IS1, IS3 and IS7) of ENVISAT ASAR data in LZG. The upper 2 picture in Fig. 12 shows the estimates of the roughness parameter (standard deviation of surface height) and soil moisture before eliminating vegetation effect in the study area. The bottom 2 pictures show the comparison between soil moisture inverted from ASAR data and ground truths at sites D and E. The proposed method is shown to be an effective method for surface roughness characterization and soil moisture mapping at regional scale, based solely on satellite data in place of using ancillary information, such as point measurements by pin-profilometer [24].

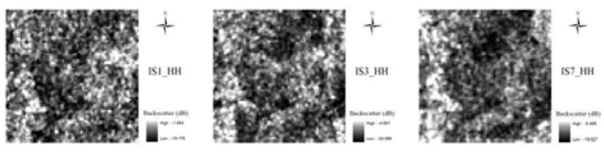

Figure 11. Subsets of the processed images from different swaths (IS1, IS3 and IS7) of the study area

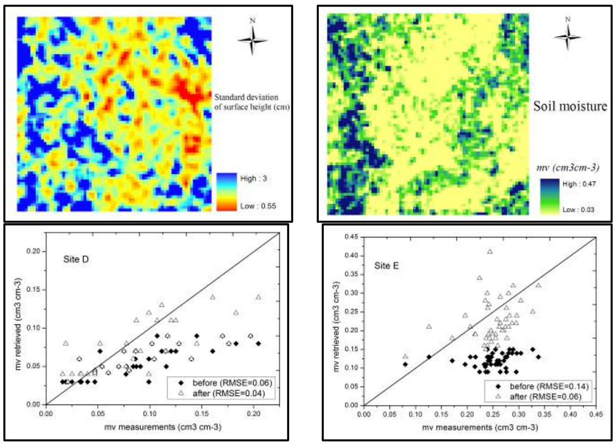

Figure 12. Estimates of surface roughness and soil moisture

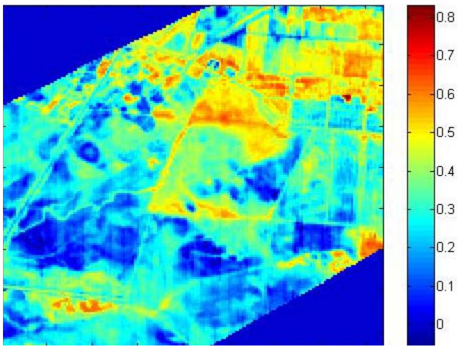

Figure13. Soil moisture (g cm^{-3}) retrieved from WiDAS in Linze Grassland Station

Retrieval of soil moisture from airborne multi-angular TIR images (WiDAS) was also attempted. This case study explored the possibility to extract soil moisture from feature space composed of TIR anisotropic factors, using WiDAS multi-angle TIR image data [25]. A linear regression relationship was built to obtain soil moisture (Fig. 13), which is

$$\text{soil moisture} = 1.3258 + 0.0552 \times \text{NDVI} + (-0.0342) \times T_{\text{nadir}} + 0.1206 \times \left(T_{\text{nadir}} - T_{30^\circ}\right) \quad (3)$$

where, T_{nadir} and $T_{30°}$ are surface temperatures measured from Nadir and 30°, respectively.

3. Biogeophysical parameters

Many progresses have been achieved in retrieval of biogeophysical parameters using WATER data. The example presented below is just a snapshot. Based on the hybrid canopy reflectance model, a new hyperspectral directional second derivative method (DSD) was proposed. DSD can remove the effect of soil background effectively. Additionally, this method can estimate LAI accurately through analyzing the canopy anisotropy. Fig. 14 shows the estimated LAI using multi-angular PROBA-CHRIS images [26].

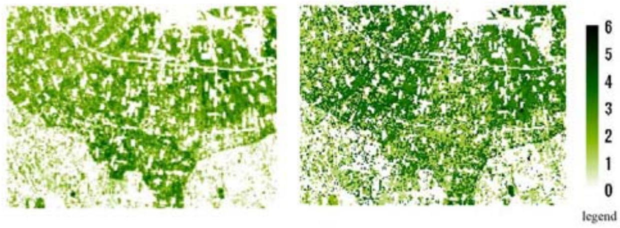

Figure 14. LAI map retrieved from an empirical relationship between LAI and NDVI (left) and using DSD (directional second derivative) method (right) from multi-angular PROBA-CHRIS data

5. SUMMARY AND PROSPECT

As an interdisciplinary, intensive, coordinated and multi-scale experiment, the data obtained from the field campaigns in WATER, both acquired from airborne and satellite-borne remote sensing, and observed on the ground, were going to be used to generate a high-resolution and spatiotemporally consistent data set for the development of integrated watershed models. The watershed science will have a more comprehensive dataset to rely on. The integrated watershed models and various algorithms to retrieve hydrological and ecological variables from remote sensing can be tested, validated, improved and later be integrated into the catchment scale land/hydrological data assimilation system, which should be capable of generating high resolution and spatiotemporal consistent data sets and thus improve the predictability of water cycle in a river basin [1].

There are many potential uses of WATER data in future. For example: (1) Combined use of WiDAS VNIR and TIR images with advanced LIDAR for the estimation of roughness parameters, (2) Further validation of the retrieval of snow properties with microwave radiometers, (3) Generalization of a roughness length algorithm over arid regions using AATSR data, (4) Combined use of AATSR based products and GRAPES data to produce meso-scale estimates of turbulent fluxes, (5) Associate LST from FengYun to produce time series of turbulent flux maps for the evaluation of the concurrent effect of water and temperature on vegetation phenology.

ACKNOWLEDGEMENTS

The ESA ENVISAT data were obtained through a grant in Dragon II program (grant number: 5322). The WATER experiment is jointly supported by the CAS Action Plan for West Development Program (grant number: KZCX2-XB2-09) and Chinese State Key Basic Research Project (grant number: 2007CB714400). We thank Dr. Shuguo Wang for acting as an editor of this report.

REFERENCES

1. Li, X., Li, X.W., Li, Z.Y., Ma, M.G., Wang, J., Xiao, Q., et. al. (2009). Watershed Allied Telemetry Experimental Research. *J. Geophys. Res*. 114, 1-19.

2. Avissar, R., & C. A. Nobre (2002). Preface to special issue on the Large-Scale Biosphere-Atmosphere Experiment in Amazonia (LBA), *J. Geophys. Res*., 107(D20), doi:10.1029/2002JD002507.

3. Goutorbe, J. P., T. Lebel, A. Tinga, P. Bessemoulin, J. Brouwer, A. J. Dolman, E. T. Engman, J. Gash, M. Hoepffner, P. Kabat, Y. H. Kerr, B. Monteny, S. Prince, F. Said, P. Sellers, & J. S. Wallace (1994). HAPEX-SAHEL - A large-scale study of land-atmosphere interactions in the semiarid tropics, *Ann. Geophys.*, 12(1), 53-64.

4. Sellers, P. J., F. G. Hall, G. Asrar, D. E. Strebel, & R. E. Murphy (1992). An overview of the 1st international satellite land surface climatology project (ISLSCP) field experiment (FIFE), *J. Geophys. Res*., D17, 18345-18371.

5. Sellers, P., F. Hall, H. Margolis, B. Kelly, D. Baldocchi, G. Denhartog, J. Cihlar, M. G. Ryan, B. Goodison, P. Crill, K. J. Ranson, D. Lettenmaier, & D. E. Wickland (1995). The Boreal Ecosystem–Atmosphere Study (BOREAS): An overview and early results from the 1994 field year, *B. Am. Meteorol. Soc.*, 76(9), 1549-1577.

6. Hu, Y. Q., Y. X. Gao, J. M. Wang, G. L. Ji, Z. B. Shen, L. S. Cheng, J. Y. Chen, & S. Q. Li (1994). Some achievements in scientific research during HEIFE, *Plateau Meteorology*, 13(3), 225-236. (in Chinese)

7. Wang, J. M. (1999). Land surface process experiments and interaction study in China – from HEIFE to IMGRASS and GAME-Tibet/TIPEX, *Plateau Meteorology*, 18(3), 280-294. (in Chinese)

8. Lü, D. R., Z. Z. Chen, J. Y. Chen, G. C. Wang, J. J. Ji, H. B. Chen, & Z. L. Liu (2005). Study on soil-vegetation-atmosphere interaction in Inner-Mongolia semi-arid grassland, *ACTA Meteorologica Sinica*, 63(5), 571-593. (in Chinese)

9. Zhang, Q., R. H. Huang, S. Wang, G. A. Wei, X. Y. Cao, X. H. Hou, S. H. Lü, Z. Y. Hu, Y. M. Ma, Z. G. Wei, Y. J. Nie, H. C. Gao, H. M. Gao, & Y. P. Yan (2005). NWC-ALIEX and its research advances, *Advance in Earth Sciences*, 20(4), 427-441. (in Chinese)

10. Cline, D., R. E. Davis, W. Edelstein, J. Hilland, K. McDonald, S. Running, J. Way, & J. van Zyl (1999). Cold Land Processed Field Experiment Plan.

11. Cheng, G. D., X. Li, E. S. Kang, Z. M. Xu, Z. T. Nan, Y. N. Zhang, X. S. Wang, & other authors, (2008). Integrated Model Development and Modeling Environment Building for Interdisciplinary Studies in the Heihe River Basin, 352 pp., Cold and Arid Regions Environmental and Engineering Research Institute, CAS, Lanzhou. (in Chinese).

12. Li, X., & Cheng, G.D. (2008). On the watershed observing and modeling systems, Advance in Earth Sciences, 23(7), 756-764. (in Chinese).

13. Li, X., Ma, M.G., Wang, J., Liu, Q., Che, T., Hu, Z.Y., Xiao, Q., Liu, Q.H., Su, P.X., Chu, R.Z., Jin, R., Wang, W. Z., & Ran, Y.H. (2007). *Watershed Airborne Telemetry Experimental Research (WATER) Implementation Plan*, 122 pp.. Cold and Arid Regions Environmental and Engineering Research Institute, CAS, Lanzhou. (in Chinese)

14. Li, X., Ma, M.G., Wang, J., Liu, Q., Che, T., Hu, Z.Y., Xiao, Q., Liu,Q.H., Su,P.X., Chu,R.Z., Jin,R., Wang,W.Z., & Ran,Y.H. (2008). Simultaneous remote sensing and ground-based experiment in the Heihe River Basin: Scientific objectives and experiment design. *Advance in Earth Sciences*. 23(9), 897-914. (in Chinese)

15. Che, T., & Li, X. (2010). Estimation of snow depth and snow water equivalent distribution using airborne microwave radiometry in the Binggou watershed, the upper reaches of the Heihe River Basin. *International Journal of Applied Earth Observation and Geoinformation*, in preparation.

16. Liang, J., & Wang, J. (2009). Hyperion hyperspectral image: Analysis and process, *Journal of Glaciology and Geocryology*, 31(2), 247-253.

17. Zhao, T. J., Zhang, L. X., Jiang, L. M., Zhao, S. J., Chai, L. N., & Jin, R. (2010). Measurement and simulation of microwave radiation from freeze-thaw soils and its monitoring using AMSR-E. *Hydrological Processes*, in review.

18. Klenk, P., Jaumann, S., Pan, X.C., Wollschlaeger, U., & Roth, K. (2010). GPR ground wave measurements of soil moisture as local ground truth for remote sensing, EGU General Assembly 2010, held 2-7 May, 2010 in Vienna, Austria, p.5444.

19. Xin, X.Z., & Liu, Q. (2010). The Two-layer Surface Energy Balance Parameterization Scheme (TSEBPS) for estimation of land surface heat fluxes. *Hydrol. Earth Syst. Sci.*, 14, 491-504.

20. Liu, Q., Yan, C. Y., Xiao, Q., Yan, G. J. & Fang, L. (2010). Separating vegetation and soil temperature using airborne multiangular remote sensing image data. *International Journal of Applied Earth Observation and Geoinformation*, submitted

21. Colin, J., Faivre, R., & Menenti, M.: Aerodynamic roughness length estimation from very high-resolution imaging LIDAR observations over the Heihe basin in China, *Hydrol. Earth Syst. Sci. Discuss.*, 7, 3397-3421, doi:10.5194/hessd-7-3397-2010.

22. Chen, K.S., Wu, T.D., Tsang, L., Li, Q., Shi, J., and Fung, A.K.: Emission of rough surfaces calculated by the integral equation method with comparison to three-dimensional moment method simulations, IEEE T. Geosci. Remote., 41, 90-101, 2003.

23. Wu, T.D., Chen, K.S., Shi, J., and Fung, A.K.: A transition model for the reflection coefficient in surface scattering, IEEE T. Geosci. Remote., 39, 2040-2050, 2001.

24. Wang, S. G., Li, X., Han, X. J., & Jin, R.: Estimation of surface soil moisture and roughness from multi-angular ASAR imagery in the Watershed Allied Telemetry Experimental Research (WATER), Hydrol. *Earth Syst. Sci. Discuss.*, 7, 3365-3396, doi:10.5194/hessd-7-3365-2010.

25. Peng, J. J., Liu, Q., Liu, Q. H. & Li, J. H. (2010). Retrieving soil moisture from air-borne multi-angle TIR image data. in preparation.

26. Fan, W.J., Xu, X.R., Liu, X.C., Yan, B.Y., & Cui, Y.K. (2010). Accurate LAI retrievel method based on PROBA/CHRIS data. *Hydrol. Earth Syst. Sci. Discuss.*, 14, 1499-1507.

Table 1. Satellite data acquired in WATER (up to 30 July, 2010)

Type	Remote sensors	Observation aims	Scale	Time	Amount
ESA	ENVISAT ASAR *	Soil freeze/thaw status, soil moisture	KEA and the whole Heihe River Bain	POP & IOP	179 scenes, ~ 45GB
	ENVISAT MERIS *	Reflectance, albedo, LST, snowcover extent, biogeophysical parameters	Whole Heihe River Bain	IOP, persistent observation period	85 scenes, ~ 1GB
	ENVISAT AATSR *	LST, ET	KEA	IOP	126 scenes, ~ 30GB
Chinese	BEIJING-1 MSI *	Snow cover extent, mapping of the experimental area	KEA	IOP	11 scenes, ~ 5GB
Third Party Mission	PROBA CHRIS *	Biogeophysical parameters, biogeochemical parameters, snow grain size	FEA	POP & IOP	23 scenes, ~ 9GB
	ALOS PRISM	Vegetation classification, mapping of the experimental area	FEA	Experiment planning period, IOP	4 scenes, ~ 1.1GB
	ALOS PALSAR	Soil freeze/thaw status, soil moisture	KEA and the whole Heihe River Bain	POP & IOP	13 scenes, ~ 15GB
Others	IKONOS	Vegetation classification, mapping of the experimental area	FEA	Experiment planning period, IOP	1 scene, 199MB
	QUICKBIRD				1 scene, 547MB
	SPOT5 HRG				3 scenes, ~ 1GB
	ASTER	Reflectance, albedo, LST, snow surface temperature, snowcover extent, biogeophysical parameters	KEA	IOP	15 scenes, ~ 6GB
	LANDSAT TM & ETM+				49 scenes, ~ 40GB
	MODIS		Whole Heihe River Bain	IOP, persistent observation period	499 scenes, ~ 34 GB
	HYPERION	Reflectance, albedo, biogeochemical parameters, snow grain size	FEA	POP & IOP	6 scenes, ~ 1.8GB
	RADARSAT-2	Snow depth, structure parameters of forest	KEA and the whole Heihe River Bain	POP & IOP	2 scenes

Note: * represents the data acquired from Dragon 2 programme